Construction and Building Materials 114 (2016) 317–322

Contents lists available at ScienceDirect

Construction and Building Materials

journal homepage: www.elsevier.com/locate/conbuildmat

Residual stress redistribution induced by fatigue in cold-drawn prestressing steel wires

J. Toribio *, M. Lorenzo, D. Vergara, L. Aguado

Fracture & Structural Integrity Research Group, University of Salamanca, E.P.S., Campus Viriato, Avda. Requejo 33, 49022 Zamora, Spain

HIGHLIGHTS

- Fatigue loading clearly reduces tensile residual stresses at the wire surface.
- This effect is even better for wires with high tensile surface residual stresses.
- Such a reduction undoubtedly improves the fatigue performance of the cold drawn wires.
- It is beneficial from the viewpoint of H embrittlement susceptibility of the wires.
- Minor fatigue-induced reduction appears in residual stresses of compressive nature.

GRAPHICAL ABSTRACT

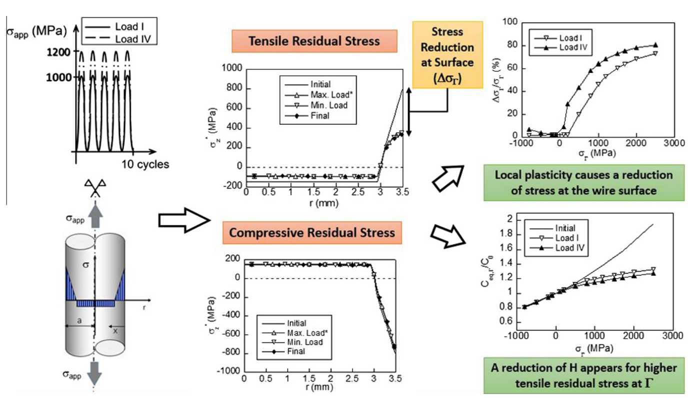

ARTICLE INFO

Article history:
Received 12 October 2015
Received in revised form 2 March 2016
Accepted 7 March 2016
Available online 2 April 2016

Keywords:
Prestressing steels
Residual stresses
Fatigue
Stress redistribution

ABSTRACT

In this paper the evolution of diverse residual stress states (similar to the ones produced after a cold drawing process) during several fatigue loading schemes is analysed. Thus, numerical simulations by finite element method were carried out applying diverse fatigue loading schemes to several cold drawn wires with a residual stress state associated. Numerical results reveal the key role of plastic strains produced by fatigue loading causing a redistribution of the residual stress when tensile stresses are placed at the wire surface. However, a negligible effect is obtained for wires with a compressive residual stress associated.

1. Introduction

Prestressing steel wires are commonly used in civil engineering as reinforcement elements for prestressed concrete structures which must bear fatigue loadings. Nowadays, cold drawing is the main conforming process used in industry for obtaining prestressing steel wires. Residual stresses appear in cold drawn wires due to the non-uniform distribution of plastic strain during the conforming process: wire drawing [1,2]. Briefly, this process consists in forcing to pass a hot rolled bar through diverse drawing dies where a progressive reduction of the wire cross sectional area is carried out [2]. As results, changes are produced at microstructural level causing a significant increment of the cold drawn wire strength [3]. Nevertheless, during drawing the wire undergoes a huge stress concentration over the vicinity of the contact zone between wire and die. Therefore, a non-uniform distribution of residual stress is produced in the wire section with a complex shape, with tensile

* Corresponding author at: Department of Materials Engineering, University of Salamanca, E.P.S., Campus Viriato, Avda. Requejo 33, 49022 Zamora, Spain.

E-mail addresses: toribio@usal.es (J. Toribio), mlorenzo@usal.es (M. Lorenzo), diego.vergara@ucavila.es (D. Vergara), laguado@usal.es (L. Aguado).

http://dx.doi.org/10.1016/j.conbuildmat.2016.03.037
0950-0618/

stresses near the contact zone and compressive stresses near the wire core [4–6]. Residual stresses of tensile nature play a key role in surface crack initiation process [7,8]. It is well-known the industrial use of different surface treatments, e.g. shot peening, which provides compressive residual stress at the material surface, thus delaying the initiation and propagation of cracks [9–12]. In addition, the synergic action of non-uniform residual stress and strain states enhances environmental induced fracture such as hydrogen embrittlement (HE) to which prestressing steel wires are particularly susceptible [13,14]. The HE of prestressing steels has been analysed profusely [2] in terms of the main stage of such a process: the hydrogen diffusion that is strongly dependent of the stress and strain state fields inside the material.

Under in-service conditions, prestressing steels wires undergo fatigue loadings. Consequently, the variables affecting the damage and fracture processes in both inert and aggressive environments vary with time. Thus, the evolution with time of the residual stress state during fatigue loading is necessary for obtaining a better knowledge regarding one of the factors involved in the damage processes and, therefore, the determination of the optimal conditions for assessing the structural integrity of prestressing steel wires. So, the aim of this paper is to analyse the evolution during several fatigue loading schemes of diverse residual stress states similar to the ones produced after a cold drawing process and the implications of such states on HE susceptibility of wires. To achieve this goal, numerical simulations by the finite element (FE) method were carried out applying diverse fatigue loading schemes to several cold drawn wires. For each one of them, an idealized residual stress state was introduced not only with a tensile state at the wire surface but also with a compressive state in that location.

2. Numerical modeling

Six different fatigue loading schemes were analysed. All of them with sinusoidal variation with time considering stress factor $R = 0$, as summarized in Table 1. This way, fatigue cycles oscillate between a null stress and a maximum stress of 1000 and 1200 MPa (i.e., about 75% and 90% of $\sigma_Y = 1300$ MPa, 0% offset yield strength of a typical prestressing steel used in construction [15]). The effect of the number of cycles (N) was included in this analysis considering three loading sequences of 10, 20 and 100 cycles. Thus, the type I represents a fatigue loading of 10 cycles with a maximum stress level of $0.75\sigma_Y$ (1000 MPa), the type II and III reaches the same maximum stress but now considering 20 and 100 cycles respectively. The type IV consists of 10 cycles with a maximum stress level of $0.9\sigma_Y$ (1200 MPa) and, finally, the schemes V and VI have a maximum stress of 1200 MPa and 20 and 100 cycles respectively.

In addition, the residual stress profiles were idealized according to the values of the surface stresses obtained experimentally by the application of diverse techniques, such as Neutron or X-ray diffraction [16–18]. Such techniques allow obtaining the stress state in samples only for a certain depth from surface. In this paper, the residual stress state after drawing was idealized considering two zones: (i) firstly a linearly decreasing stress from the wire surface up to a point whose depth from surface is equivalent to the one given by diffraction techniques and, secondly, a constant stress distribution up to the wire core. The value of the stress distribution over the second zone can be obtained applying the equilibrium condition to the stress state over the whole cross sectional area of the wire in terms of the second Pappus-Guldin Theorem [19]. This approach allows one to reproduce the general shape of the residual stresses profiles observed with the most commonly used measurement techniques without any loss of generality.

Table 1
Number of cycles and maximum stress level applied in the different fatigue loading considered.

Fatigue Loading Schemes	I	II	III	IV	V	VI
σ_{max} (MPa)	1000	1000	1000	1200	1200	1200
N	10	20	100	10	20	100

Thirteen residual stress profiles were analysed in the present study which can be divided, according to the nature of the surface wire stress, into tensile residual stress states (profiles 1, 3, 5, 7 and 9–13 in Table 2) and compressive residual stress states (profiles 2, 4, 6 and 8 in Table 2). The idealized residual stress profiles can be defined by using just two parameters: the maximum residual stress level at the surface, σ_Γ, and the depth x_0 (x being the distance from the wire surface) where the stresses reach a constant value, as depicted in Fig. 1.

The simulation of the fatigue loading applied to the prestressing steel wire is carried out by FE using a commercial code (MSC.Marc). Due to the axisymmetric geometry of the wire, the three-dimensional (3D) case is simplified to an equivalent two-dimensional (2D) problem. Consequently, a fixed displacement in the radial direction was applied at the nodes placed at the symmetry axis of the wire (Fig. 2). In addition, a null displacement in the axial direction was imposed at nodes located at the transversal cross section of the wire (Fig. 2) due to symmetry of both fatigue loading and geometry of the wire. This way, only a half of the wire is needed in modelling with important saving of computing time in simulations. Finally, a fatigue loading (σ_{app}) corresponding to each case of study according to the parameters of the fatigue loading included in Table 1 was applied at the opposite edge of the wire (Fig. 2).

In order to reproduce the idealized residual stress profile, the meshing of the wire was carried out considering progressively increased size of the elements with wire depth (Fig. 2) [20]. Thus, close to the wire surface, the profile exhibits the most significant variations and hence the mesh of the wire is more refined. On the contrary, out of this zone a constant distribution is considered and, therefore, a coarse mesh was applied. This way a more accurate approach to the theoretical stress profile can be achieved by assigning to each element an initial stress value which depends on the distance to the wire surface, as shown in Fig. 2 where these initial stress values (constant in each finite element) are plotted in comparison with the exact profile previously described. The meshing of the geometry is developed with four nodes quadrilateral elements due to the simple geometry of the wire. The constitutive model for the material was chosen to be elasto-plastic with isotropic strain hardening rule given by the master stress and strain curve obtained experimentally from a standard tensile test. Results provide the following material properties: Young modulus, $E = 200$ GPa and 0% offset yield stress, $\sigma_Y = 1300$ MPa.

3. Influence of the loading scheme

The evolution with time (simulation time t) of axial stress at two different depths was analysed. Each one of them represents the two zones in which the idealized residual stress profile was divided (cf. Fig. 1). Thus, the first one is placed at the wire surface where the maximum stress is located, and the second one is placed at the middle of the zone with uniform stress (cf. Fig. 1). Due to a lack of space, only the evolutions of axial stress at the three last cycles for two wires are shown in Fig. 3: (i) profile 7 ($\sigma_\Gamma = 800$ MPa), representing the tensile residual profiles; (ii) profile 8 ($\sigma_\Gamma = -800$ MPa), representing the compressive stress profiles. In both cases t represents the dimensionless simulation time.